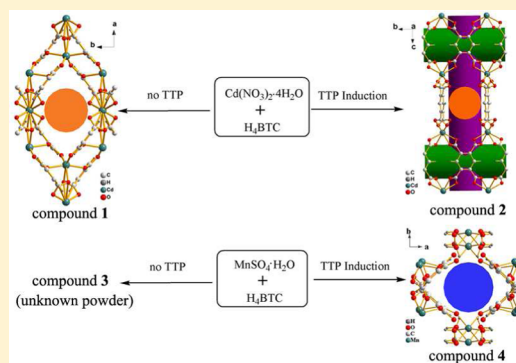


Structural Induction Effect of a Zwitterion Pyridiniumolate for Metal–Organic Frameworks

Jian Su,[†] Liudi Yao,^{†,§} Meng Zhao,[†] Hui Wang,[†] Qiong Zhang,[†] Longjiu Cheng,[†] Jun Zhang,^{*,†,‡} Shengyi Zhang,[†] Jieying Wu,[†] and Yupeng Tian^{*,†}[†]Department of Chemistry, Key Laboratory of Functional Inorganic Materials Chemistry of Anhui Province, Anhui University, Hefei 230039, P. R. China[‡]Key Laboratory of Functional Molecule Design and Interface Process, Anhui Jianzhu University, Hefei 230601, P. R. China[§]Institution of Technology, Tallaght, Dublin 24, Ireland

S Supporting Information

ABSTRACT: It is still an enormous challenge to obtain the metal–organic frameworks (MOFs) with specific properties by tuning their structures. Here we first reported that the structures of MOFs could be tuned by adding certain amount of zwitterion pyridiniumolate. To demonstrate the inductive effect, two series of assembly experiments were performed using different metal ions, namely, Cd(II) and Mn(II). The experimental results revealed that the zwitterion pyridiniumolate only acted as a structural induction agent (SIA), which did not exist in the aimed compounds. The SIAs could effectively tune the framework aperture or promote coordination and further tune the properties of MOFs without any removal or exchange after the synthesis. Therefore, the results could not only immensely expand the syntheses and structural diversity of MOFs with the fixed metal ions and organic ligands but also afford the possibility and effective convenience for tuning the properties of MOFs in the functional material research fields.



INTRODUCTION

Metal–organic frameworks (MOFs) have attracted considerable attention due to the vast variety of interesting structural topologies as well as their potential applications in gas separation,¹ catalysis,² nonlinear optics,³ and so forth. Although thousands of MOFs have been synthesized, the tuning of MOF structures, which are closely related to their properties, remains an enormous challenge.⁴ Designing and applying new organic ligands are the common ways to construct specific functional MOF materials. Yaghi et al. have conducted a groundbreaking work in tuning the scale of apertures of MOF channels by controlling the length and width of organic linkers.⁵

It is known that during the synthesis of zeolites, which are the most crucial solid catalysts,⁶ some organic molecules are applied as templates for tuning the structures of the zeolites;⁷ the templates, included in the cavities/channels of the products, must be removed by intensive heating, which tends to destroy the original structures. Recently, templates and structural direct agents (SDAs) were widely used to obtain various MOF structures.⁸ Although there is no exact distinction between templates and SDAs, after reading the related reported works, they both have drawbacks, which can be listed as follows: (a) it is not easy to be removed or exchanged after the synthesis. That is to say, agents tend to coordinate to the metal ions or stay in the cavities/channels in the MOF structures; (b) the classes of these matters are limited in organic amines, some

solvents, inorganic templates, and other surfactants.⁹ In this perspective, new kinds of matters we called structural induction agents (SIAs) with the description of “matters necessarily exist in the synthetic system and have important roles to form structures of the aimed compounds, while they have neither coordination actions with the metal ions nor stay in the cavities/channels of the resultant frameworks” are pressingly requested.

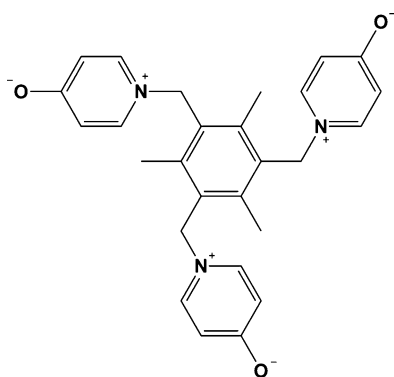
To the best of our knowledge, only camphoric acid was reported with the function of SIAs.¹⁰ To found novel SIAs was just our interest. In this work, a zwitterion pyridiniumolate, 1,1',1''-(2,4,6-trimethylbenzene-1,3,5-triyl)tristripyridinium-4-olate (TTP, Scheme 1), a completely new SIA, was first reported to induce the frameworks. Several novel MOFs were constructed and confirmed the inductive effect of TTP as an SIA (as shown in Figure 1) with Cd²⁺/Mn²⁺ and benzene-1,2,4,5-tetracarboxylic acid (H₄BTC) in the parallel conditions. Here, we report the inductive effect of TTP as a novel SIA, as well as the synthesis, structural analysis, and semiconductor and photoluminescence properties of those MOFs.

Received: January 29, 2015

Published: June 5, 2015



Scheme 1. Structure of the TTP as a Structural Induction Agent



EXPERIMENTAL SECTION

Materials and Methods. All the reagents and solvents were commercially available and used as received. FT-IR was performed on VERTEX 80 with KBr pellets from 4000 to 400 cm^{-1} . Elemental analyses (EA) for C, H, and N were measured on Vario ELIII. The powder X-ray diffraction patterns (PXRD) were recorded on a Bruker Advance D8 (40 kV, 40 mA) diffractometer (Cu radiation, $\lambda = 1.54056 \text{ \AA}$) with a scan speed of 0.5 s/deg at room temperature. Thermogravimetric analysis (TGA) data were performed under N_2 atmosphere using a TGA-50 (SHIMADZU) thermogravimetric analyzer at $10^\circ\text{C min}^{-1}$. The solid-state luminescence spectra were given by F-4500 FL spectrophotometer (EX slit: 10.0 nm, EM slit: 10.0 nm, PMT voltage: 500 V). Diffuse reflectance spectrum was obtained by a U-41000 Spectrophotometer applying BaSO_4 powder as a 100% reflectance reference.

X-ray Structure Studies. Data were obtained on a Bruker Smart APEX II diffractometer with a CCD area detector at room temperature. Raw data were collected and reduced using APEX2 software.¹¹ Adsorption corrections were performed by the SADABS program. The structures of compounds 1, 2, and 4 were originally solved by direct methods and then refined by full-matrix least-squares on F^2 applying the SHELXTL software.¹² All non-hydrogen atoms were refined with anisotropic displacement parameters. All hydrogen atoms of H_4BTC ligand were calculated in ideal positions and then refined with isotropic displacement parameters. The water molecules

and dimethylammonium cations resulting from dimethylformamide (DMF) hydrolysis¹³ for compounds 1 and 4 were observed from electron density peaks and then refined with restrictions. Free dimethylammonium cations and water molecules of compound 2 were highly disordered and were unsuccessfully located and refined. The diffuse electron densities of these residual solvents were removed from the data set by the SQUEEZE routine of PLATON software, and then the generated data were used to further refine the structure.¹⁴ The unit cell contents did not represent the solvent region. The final formula of compound 2 was obtained by the calculation from the SQUEEZE results and simultaneously compared with elemental analysis, charge balance, and TGA data.

Crystal Data for 1. $\text{C}_{24}\text{H}_{22}\text{O}_{17}\text{Cd}_3\text{N}_2$, FW = 947.64, orthorhombic, space group $Ibam$, $a = 20.745(2) \text{ \AA}$, $b = 8.3255(8) \text{ \AA}$, $c = 17.3435(17) \text{ \AA}$, $V = 2995.5(5) \text{ \AA}^3$, $Z = 4$, $d_{\text{calcd}} = 2.101 \text{ g}^{-3}$, $R_1(I > 2\sigma(I)) = 0.0448$, wR_2 (all data) = 0.1956, GOF = 1.055. **2:** $\text{C}_{14}\text{H}_{20}\text{O}_9\text{CdN}_2$, FW = 472.73, tetragonal, space group $P4_2/mbc$, $a = b = 13.795(2) \text{ \AA}$, $c = 17.743(6) \text{ \AA}$, $V = 3376.4(14) \text{ \AA}^3$, $Z = 8$, $d_{\text{calcd}} = 1.426 \text{ g}^{-3}$, $R_1(I > 2\sigma(I)) = 0.0425$, wR_2 (all data) = 0.1634, GOF = 1.055; **4:** $\text{C}_{24}\text{H}_{30}\text{O}_{22}\text{Mn}_3\text{N}_2$, FW = 863.32, orthorhombic, space group $Pbcn$, $a = 19.1035(9) \text{ \AA}$, $b = 9.5430(4) \text{ \AA}$, $c = 17.6708(8) \text{ \AA}$, $V = 3221.5(3) \text{ \AA}^3$, $Z = 2$, $d_{\text{calcd}} = 1.780 \text{ g}^{-3}$, $R_1(I > 2\sigma(I)) = 0.0284$, wR_2 (all data) = 0.0773, GOF = 1.036; additional crystallographic information is available in the Supporting Information.

Synthesis of TTP. TTP was prepared adopting the procedure reported by Zhang et al.¹⁵

Synthesis of Compound 1: $[(\text{BTC})\text{Cd}] \cdot (\text{H}_2\text{O}) \cdot (\text{CH}_3\text{NH}_2\text{CH}_3)_2$. The solid of $\text{Cd}(\text{NO}_3)_2 \cdot 4\text{H}_2\text{O}$ (0.060 g, 0.19 mmol) was solved in the solution of H_4BTC (0.024 g, 0.095 mmol) in 4 mL of DMF and 1 mL of H_2O , to which two drops of 6 mol/L HCl were added. The mixture was sealed in a vial and heated to 100°C in a drying oven for 72 h, then cooled to room temperature. The colorless block crystals (0.036 g) of 1 were collected by filtration and dried in the air after washing with DMF and CH_2Cl_2 three times, respectively. Yield 79.98% (based on H_4BTC). Anal. Calcd for $\text{C}_{24}\text{H}_{24}\text{O}_{18}\text{Cd}_3\text{N}_2$ ($M_r = 947.64$): C, 30.24; H, 2.34; N, 2.96%. Found: C, 30.20; H, 2.54; N, 2.63%. FT-IR (KBr pellet, cm^{-1}): 3459 m, b, 3064 m, b, 2935 w, 2796 w, 2513 w, 2449 w, 2373 w, 1660 s, 1610 s, 1589 s, 1540 vs, 1492 s, 1371 vs, 1323 s, 1245 m, 1184 m, 1138 m, 1105 m, 1016 m, 958 w, 871 m, 815 m, 769 m, 751 m, 615 m, 565 m, 526 m.

Synthesis of Compound 2: $[(\text{BTC})\text{Cd}] \cdot (\text{H}_2\text{O}) \cdot (\text{CH}_3\text{NH}_2\text{CH}_3)_2$. The solid of $\text{Cd}(\text{NO}_3)_2 \cdot 4\text{H}_2\text{O}$ (0.060 g, 0.19 mmol) was solved in the solution of H_4BTC (0.024 g, 0.095 mmol) and TTP (0.044 g, 0.100

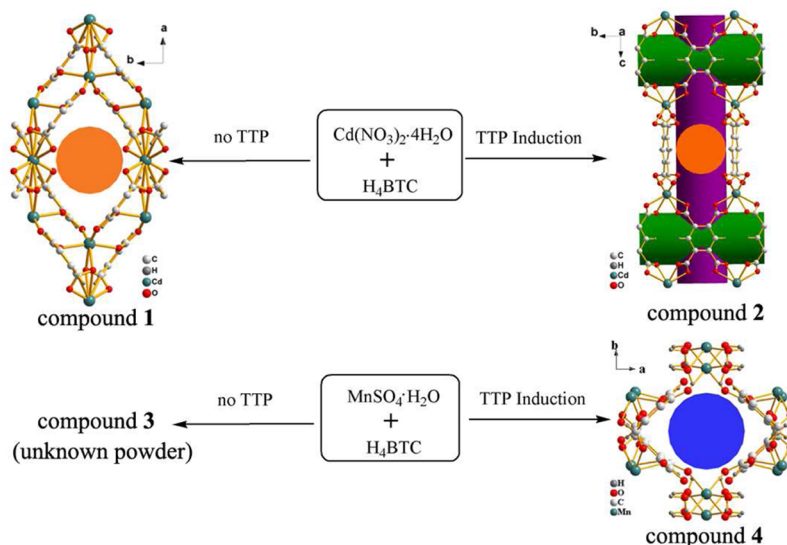


Figure 1. Illustration of the structural induction effect of TTP in the syntheses of compounds 1, 2, 3, and 4. Compounds 2 and 4 were synthesized in the presence of TTP, while 1 and 3 were prepared in the absence of TTP. TTP existed in neither the frameworks nor the cavities/channels of compounds 2 and 4; it only acted as SIA in the synthetic systems.

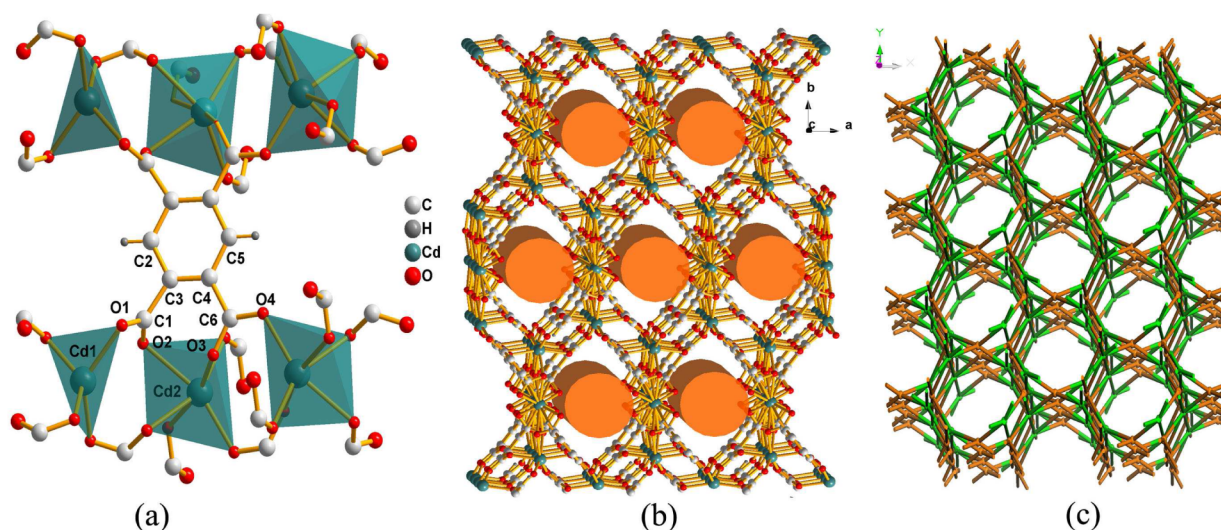


Figure 2. (a) The coordination environment of BTC⁴⁻ and Cd ions in compound 1. (b) The ball-and-stick views of the microporous frameworks of compound 1. (c) Topological representations of compound 1 with stoichiometry of $\{4^4\cdot6^2\}\{4^5\cdot6\}_2\{4^7\cdot6^6\cdot8^2\}_2$.

mmol) in 4 mL of DMF and 1 mL of H₂O, to which two drops of 6 mol/L HCl were added. The mixture was sealed in a vial and heated to 100 °C in a drying oven for 72 h, then cooled to room temperature. The colorless octahedral crystals (0.040 g) of **2** were collected by filtration and dried in the air after washing with DMF and CH₂Cl₂ three times, respectively. Yield 88.14% (based on H₄BTC). Anal. Calcd for C₁₄H₂₀O₉CdN₂ (*M_r* = 472.73): C, 35.57; H, 4.26; N, 5.92%. Found: C, 35.18; H, 4.07; N, 5.62%. FT-IR (KBr pellet, cm⁻¹): 3433 m, b, 3184 w, 3102 w, 2800 m, 2501 w, 1564 s, 1493 vs, 1427 s, 1386 vs, 1323 s, 1138 m, 1018 m, 923 w, 873 s, 829 s, 767 m, 679 m, 565 m, 528 m, 449 m.

Synthesis of Compound 4: [(BTC)₂(H₂O)₄Mn₃]·(H₂O)₂·(CH₃NH₂CH₃)₂. The solid of MnSO₄·H₂O (0.016 g, 0.097 mmol) was solved in the solution of H₄BTC (0.012 g, 0.048 mmol) and TTP (0.022 g, 0.100 mmol) in 4 mL of DMF and 1 mL of H₂O, to which two drops of 6 mol/L HCl were added. The mixture was sealed in a vial and heated to 100 °C in a drying oven for 72 h, then cooled to room temperature. The colorless block crystals (0.017 g) of **4** were collected by filtration and dried in the air after washing with DMF and CH₂Cl₂ three times, respectively. Yield 82.05% (based on H₄BTC). Anal. Calcd for C₂₄H₃₀Mn₃N₂O₂₂ (*M_r* = 863.32): C, 33.39; H, 3.50; N, 3.24%. Found: C, 33.22; H, 3.47; N, 3.51%. FT-IR (KBr pellet, cm⁻¹): 3421m, b, 3081 m, b, 2968 w, 2852 w, 2800 w, 2501 w, 2356 w, 1591 vs, 1489 w, 1469 w, 1369 s, 1354 s, 1244 w, 1138 m, 1115 m, 1024 m, 896 w, 869 w, 794 m, 727 w, 617 m, 464 w.

RESULTS AND DISCUSSION

Synthesis. In the current work, we first present two novel MOFs (**1** and **2**), which were both obtained by the assembly of Cd(NO₃)₂·6H₂O and H₄BTC in DMF/H₂O under the same solvothermal synthetic conditions except that an addition of TTP was made during the synthesis of compound **2**. Interestingly, TTP acting as SIA can effectively tune the coordination modes of polycarboxylate ligands to enhance the pore volume ratio. To demonstrate that the structural induction effect reported here could be extended to another system, Cd²⁺ was replaced with Mn²⁺. Unknown powder **3** appeared in the absence of TTP, while crystals of compound **4** were obtained in the presence of TTP under the same synthetic conditions. Overall, these compounds clearly demonstrated the structural induction effect of TTP (as shown in Figure 1). To give a deep knowledge of the structural induction effect, we give a reasonable speculation regarding the structural induction factor because of the uncertainty of the TTP configuration in

solutions, or in the reported MOF structures.¹⁵ However, when triangular TTP was replaced with quadrangular or other shaped zwitterion pyridiniumolates in the synthetic system, the inductive effect still emerged. So, we think the factor is the nature of zwitterion of TTP. In brief, we found a new kind matter in a simple and effective way to obtain various frameworks with the fixed metal salts and organic ligands at the parallel reaction conditions just by adding an SIA.

Crystal Structure. In the structure of compound **1**, as shown in Figure 2a, the Cd1 adopts a distorted tetrahedron CdO₄ coordination geometry and is coordinated by four carboxylates from four different BTC⁴⁻ ligands in monodentate mode, while Cd2 adopts a distorted octahedron CdO₆ coordination geometry and is coordinated in monodentate mode by six carboxylates from four different BTC⁴⁻. The BTC⁴⁻ ligand applies its four carboxylate groups to coordinate with six Cd ions in monodentate mode. The Cd–O interatomic distances range from 2.226(3) to 2.639(3) Å, and O–Cd–O angles range from 53.03(9) to 168.84(1)°, consistent with those reported for other Cd-carboxylate complexes.¹⁶

The three-dimensional (3D) framework of compound **1** is constructed from a 3D hexagonal prism building unit (Supporting Information, Figure S13a). Within the 3D structure (Figure 2c), the maximum diagonal distance of the opening sizes for the rhomboid topological channels along the *c* direction is ca. 4.91 × 9.57 Å². The total solvent-accessible volume calculated by PLATON¹⁴ based on the crystal structure is ~1079.9 Å³ per unit cell, possessing 36.1% of the total crystal volume. In the topological view, compound **1** can be built from a four-connected Cd1 ion, a six-connected Cd2 ion, and a four-connected BTC⁴⁻ ligand. Each Cd ion is connected by four BTC⁴⁻ ligands, while each BTC⁴⁻ ligand is connected by four Cd ions. This results in a trinodal (4, 4, 6)-connected FSI topology (Figure 2c). The four-connected Cd1 node, six-connected Cd2 node, and the BTC⁴⁻ node have the point symbol of {4⁴·6²}, {4⁵·6}, and {4⁷·6⁶·8²}, respectively. So, the topological network of compound **1** can be represented as a trinodal (4, 4, 6) net with the stoichiometry of {4⁴·6²}{4⁵·6}₂{4⁷·6⁶·8²}.¹⁷

By adding a suitable amount of TTP, a different structure of compound **2** with Cd²⁺ and BTC⁴⁻ was obtained. As shown in

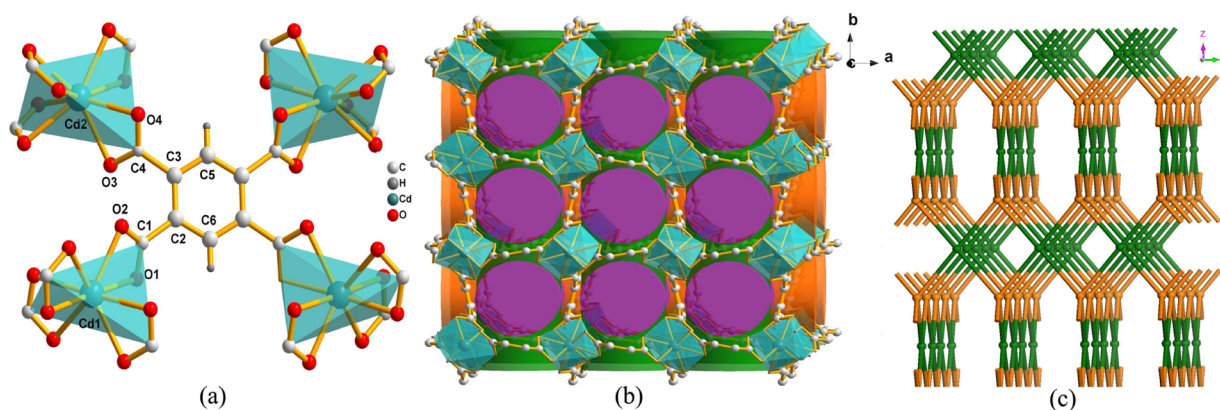


Figure 3. (a) The coordination environment of BTC⁴⁻ and Cd ions in compound **2**. (b) The ball-and-stick views of the microporous frameworks of compound **2**. (c) Topological representations of compound **2** with stoichiometry of {4²·8²}.

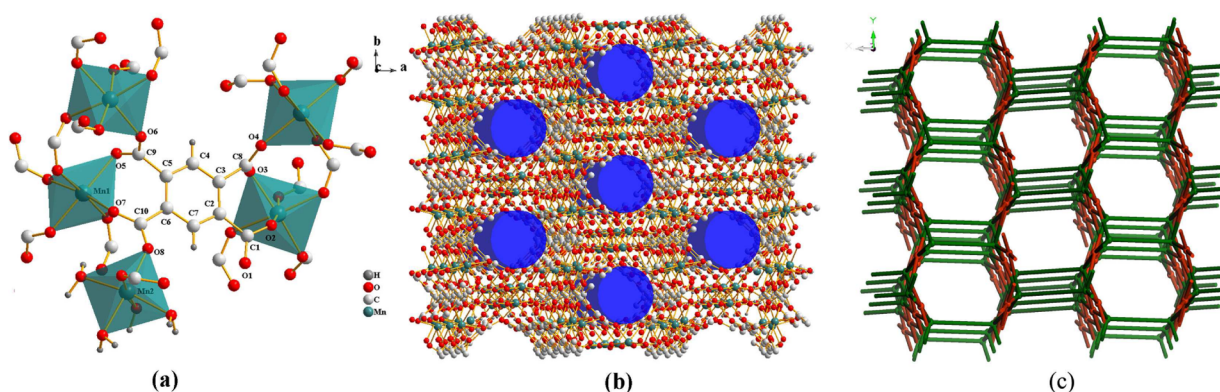


Figure 4. (a) The coordination environment of BTC⁴⁻ and Mn ions in compound **4**. (b) The ball-and-stick views of the microporous frameworks of compound **4**. (c) Topological representations of compound **4** with stoichiometry of {4⁴·6²} {4⁴·6⁶}.

Figure 3a, the Cd ion is coordinated by four carboxylates from the four different BTC⁴⁻ ligands, giving rise to a distorted tetrahedron Cd(COO)₄. The BTC⁴⁻ ligand applies its four carboxylate groups to coordinate with four Cd ions in chelating mode. The Cd–O bond lengths and O–Cd–O angles are within normal ranges, respectively.¹⁶ The 3D structure of compound **2** is built from a 3D rectangular building unit (Supporting Information, Figure S13b). Within the 3D structure (Figure 3b), the rectangular topological channels run along the crystallographic *a*, *b*, and *c* directions with maximum opening sizes of ca. 3.35 × 5.47, 3.35 × 5.47, and 4.26 × 4.26 Å², respectively. The total solvent-accessible volume calculated by PLATON¹⁴ is ~1492.6 Å³ per unit cell, possessing 44.2% of the total crystal volume. Note that compound **2** is more porous than compound **1** demonstrating the potential application of the induction agent to improve the MOF properties. From the viewpoint of topology, compound **2** can be built from a four-connected Cd ion and a four-connected BTC⁴⁻ ligand. Each Cd ion is connected by four BTC⁴⁻ ligands, while each BTC⁴⁻ ligand is connected by four Cd ions. This results a common binodal (4, 4)-connected PtS topological network (Figure 3c). The four-connected Cd node and BTC⁴⁻ node possess the same point symbol of {4²·8²}.¹⁷ So, the topological network of compound **2** can be represented as a binodal (4, 4) net with stoichiometry of {4²·8²}.

In the structure of compound **4**, which was synthesized by introducing TTP and different from unknown power **3** without TTP, BTC⁴⁻ is coordinated to five Mn²⁺ ions with two of its four carboxylate groups in chelating mode and two of them in

monodentate mode (Figure 4a). The Mn–O interatomic distances range from 2.1144(1) to 2.2331(1) Å, and O–Mn–O angles range from 81.23(5) to 177.05(6)°, consistent with those reported Mn-carboxylate complexes.¹⁸ Within the 3D structure (Figure 4b), the maximum diagonal distance of the opening sizes for the rectangular topological channels along *c* direction is ca. 5.53 × 4.97 Å². The total solvent-accessible volume calculated by PLATON¹⁴ is ~954.2 Å³ per unit cell, possessing 29.6% of the total crystal volume. In a topological view, compound **4** can be built from a four-connected Mn1 ion and a five-connected BTC⁴⁻ ligand (Figure 4c). So, the topological network of **4** can be regarded as a binodal (4, 5) net with stoichiometry of {4⁴·6²} {4⁴·6⁶}.

Thermogravimetric and Powder X-ray Diffraction Analyses.

Thermogravimetric analysis of compound **1** (see Supporting Information, Figure S1) revealed a weight loss of 1.8% (calcd 1.9%) from room temperature (r.t.) to ca. 140 °C, which is assigned to the release of guest water molecules, and the weight loss in the range of ca. 140–310 °C, which is assigned to the removal of the guest dimethylammonium molecules (exptl 7.0%; calcd 9.7%). Then it started to lose its ligands as a result of thermal decomposition. The residue is probably metal Cd (exptl 35.4%; calcd 35.6%) at ca. 480 °C. The thermogram of compound **2** (see Supporting Information, Figure S2) showed a weight loss of 2.4% (calcd 3.8%) from r.t. to ca. 140 °C, which is assigned to the release of guest water molecules, and the weight loss in the range of ca. 140–310 °C, which is assigned to the removal of guest dimethylammonium molecules (exptl 16.8%; calcd 19.5%). Above ca. 310 °C, the

framework of compound **2** started to decompose. At ca. 430 °C, the residue (52.9%) probably consisted of CdO (calcd 27.2%) and carbon; the carbon was subsequently lost above 430 °C, and the line falls very slowly. The TGA curve of compound **4** (see Supporting Information, Figure S3) showed a weight loss of 2.6% (calcd 3.1%) from r.t. to ca. 120 °C, which is assigned to the release of guest water molecules, and the weight loss in the range of ca. 120–260 °C was assigned to the removal of coordinated water molecules (exptl 7.5%; calcd 8.4%). Above ca. 260, the guest dimethylammonium molecules were lost, and the framework of compound **4** started to decompose simultaneously.

The phase purity of compounds **1**, **2**, and **4** were confirmed by PXRD measurement in which the experimental diffraction peaks were in excellent agreement with the fitted data based on single-crystal X-ray data using TOPAS¹⁹ program; moreover, the best-fitted unit cell parameters were in agreement with the single-crystal data (see Supporting Information, Figure S6). The thermal studies revealed that the frameworks of all the three compounds were probably unstable upon removal of the guest molecules, owing to no perfect platforms of compounds **1**, **2**, and **4** to be found. The stabilities of the frameworks were further checked by powder X-ray diffraction patterns (Supporting Information, Figure S5). The samples were treated at 100 °C for 12 h, and then the powder X-ray diffractions were performed. Most peaks completely disappeared so that many sections were approximately flat. Only a few peaks remained, and they were very weak or badly matched the calculated patterns. Those confirmed the enormous changes and instabilities of the frameworks after the thermal treatments. Moreover, the residual dimethylammonium ions possessed some space of the cavities/channels. Therefore, the surfaces of the three compounds from N₂ gas adsorption measurements were not obtained.

Semiconductor Behavior of Compounds **1**, **2**, and **4**.

Experimental measurements of photoluminescence or UV–vis spectroscopy showed that MOF-5²⁰ was a semiconducting compound with a band gap of ~3.4 eV, which was also confirmed by the calculations based on density functional theory.²¹ We studied the semiconducting properties of compounds **1**, **2**, and **4** by diffuse reflectance spectrum in Tauc plots (Figure 5). The results indicate that compounds **1**,

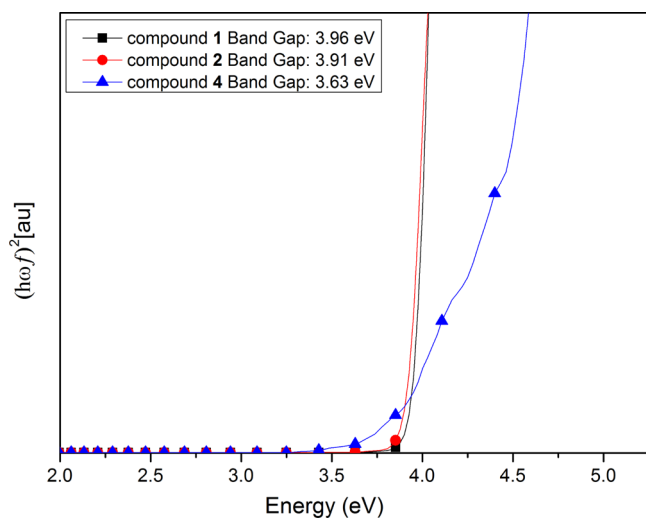


Figure 5. Tauc plots of compounds **1**, **2**, and **4**.

2, and **4** are wide-gap semiconductors with band gaps of 3.96, 3.91, and 3.63 eV, respectively. The band gap of compound **1** is wider than the band gaps of compounds **2** and **4**, which is identical with the simulated band gaps (Supporting Information, Figures S7–S9). These band gaps are comparable to that of the reported MOF-5.²⁰

Photoluminescence Property. The solid-state photoluminescence properties of **L** ligand (H₄BTC) and compounds **1**, **2**, and **4** were studied at room temperature (Figure 6). Upon

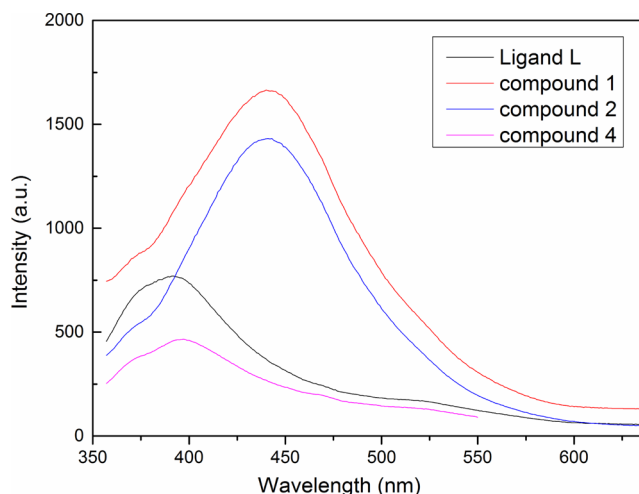


Figure 6. Solid-state emission spectra of **L** and compounds **1**, **2**, and **4** at ambient temperature (excited at 335 nm).

excitation at 335 nm, **L** ligand and compounds **1**, **2**, and **4** exhibited photoluminescence with emission bands at 391, 440, 443, and 397 nm, respectively. The emission band of the free ligand was attributed to the $\pi^* \rightarrow n$ or $\pi^* \rightarrow \pi$ transition.²² Compared with the free **L** ligand, the emission band locations of compounds **1** and **2** were red-shifted by ~50 nm, which may be assigned to ligand-to-ligand charge transfer (LLCT).²³ The red shift and increase of the band height may be attributed to the coordination effect of the ligands to Cd ions, which increased the structural rigidity and reduced the nonradiative decay of the intraligand.²⁴ The emission of compound **4** can be assigned tentatively to the coexistence of intraligand fluorescent emissions and LMCT.²³ The decrease of the peak height probably resulted from the single electron of Mn(II).²⁵

CONCLUSION

In summary, we first reported that TTP could be applied as a completely new SIA to tune the resultant frameworks for MOFs. Several MOFs with difference spatial structures were successfully synthesized. According to the parallel syntheses, the presence of TTP could change the resulting structure and improve the pore volume ratio from 36.1% to 44.2% for compounds **1** and **2** or promote the coordination progress for compounds **3** and **4**. The current study highlighted the effective tuning of MOF structures and hence opened new avenues for MOF structure tuning by TTP or the other kinds of SIAs. The method can immensely expand the syntheses and structural diversities of MOFs and can therefore increase the possibilities for scientist to obtain specific properties by effectively tuning the structures.

■ ASSOCIATED CONTENT

■ Supporting Information

PXRD setup and patterns, CIF file for compounds **1**, **2**, and **4**, TGA data, related calculation results of photoluminescence and semiconducting properties, and additional pictures of compounds **1**, **2**, and **4**. The Supporting Information is available free of charge on the ACS Publications website at DOI: 10.1021/acs.inorgchem.5b00180. CCDC 1010179 (**1**), 1010180 (**2**), and 1010181 (**4**) contain the supplementary crystallographic data for this paper. These crystal data can be obtained free of charge from The Cambridge Crystallographic Data Centre through www.ccdc.cam.ac.uk/data_request/cif.

■ AUTHOR INFORMATION

Corresponding Authors

*E-mail: zhangjun@ahjzu.edu.cn. (J.Z.)

*E-mail: yptian@ahu.edu.cn. (Y.-P.T.)

Author Contributions

J.S. and L.Y. contributed equally.

Notes

The authors declare no competing financial interest.

■ ACKNOWLEDGMENTS

The authors are thankful for the help of Prof. H. Du of Nanjing Univ., Prof. M. Fang of Nanjing Normal Univ., and Dr. X. Tian of Anhui Univ. This work was supported by the National Natural Science Foundation of China (Grant Nos. 21201005, 21271004, 21275006, 21273008, and 51372003), the Natural Science Foundation of Anhui Province (Grant Nos. 1308085QB33 and 1208085MB22), and the China Postdoctoral Science Foundation Funded Project (Grant No. 2013M541810). The calculations were performed at the HPC Center of USTC.

■ REFERENCES

- (1) (a) Li, J. R.; Kuppler, R. J.; Zhou, H. C. *Chem. Soc. Rev.* **2009**, *38*, 1477–1504. (b) Lee, K.; Isley, W. C., 3rd; Dzubak, A. L.; Verma, P.; Stoneburner, S. J.; Lin, L. C.; Howe, J. D.; Bloch, E. D.; Reed, D. A.; Hudson, M. R.; Brown, C. M.; Long, J. R.; Neaton, J. B.; Smit, B.; Cramer, C. J.; Truhlar, D. G.; Gagliardi, L. *J. Am. Chem. Soc.* **2014**, *136*, 698–704.
- (2) (a) Zhao, M.; Ou, S.; Wu, C. D. *Acc. Chem. Res.* **2014**, *47*, 1199–1207. (b) Lee, J.; Farha, O. K.; Roberts, J.; Scheidt, K. A.; Nguyen, S. T.; Hupp, J. T. *Chem. Soc. Rev.* **2009**, *38*, 1450–1459. (c) Dang, D.; Wu, P.; He, C.; Xie, Z.; Duan, C. *J. Am. Chem. Soc.* **2010**, *132*, 14321–14323.
- (3) (a) Wang, C.; Zhang, T.; Lin, W. *Chem. Rev.* **2012**, *112*, 1084–1104. (b) Evans, O. R.; Lin, W. *Acc. Chem. Res.* **2002**, *35*, 511–522.
- (4) (a) Zhang, Z.; Zaworotko, M. J. *Chem. Soc. Rev.* **2014**, *43*, 5444–5455. (b) Zhang, X.-j.; Li, J.-q.; Liu, S.-j.; Luo, M.-b.; Xu, W.-y.; Luo, F. *CrystEngComm* **2014**, *16*, 5216–5220. (c) Zhang, M.; Bosch, M.; Gentle, I.; Zhou, H.-C. *CrystEngComm* **2014**, *16*, 4069–4083. (d) Zhou, H. C.; Long, J. R.; Yaghi, O. M. *Chem. Rev.* **2012**, *112*, 673–674. (e) Cohen, S. M. *Chem. Rev.* **2012**, *112*, 970–1000.
- (5) (a) Deng, H.; Grunder, S.; Cordova, K. E.; Valente, C.; Furukawa, H.; Hmadeh, M.; Gandara, F.; Whalley, A. C.; Liu, Z.; Asahina, S.; Kazumori, H.; O’Keeffe, M.; Terasaki, O.; Stoddart, J. F.; Yaghi, O. M. *Science* **2012**, *336*, 1018–1023. (b) Rosi, N. L.; Eckert, J.; Eddaoudi, M.; Vodak, D. T.; Kim, J.; O’Keeffe, M.; Yaghi, O. M. *Science* **2003**, *300*, 1127–1129.
- (6) Corma, A. *Chem. Rev.* **1995**, *95*, 559–614.
- (7) (a) Kim, S.-S.; Shah, J.; Pinnavaia, T. J. *Chem. Mater.* **2003**, *15*, 1664–1668. (b) Bull, L.; Villaescusa, L. A.; Teat, S. J.; Cambor, M. A.; Wright, P. A.; Lightfoot, P.; Morris, R. E. *J. Am. Chem. Soc.* **2000**, *122*, 7128–7129. (c) Choi, M.; Cho, H. S.; Srivastava, R.; Venkatesan, C.; Choi, D. H.; Ryoo, R. *Nat. Mater.* **2006**, *5*, 718–723. (d) Xiao, F. S.; Wang, L.; Yin, C.; Lin, K.; Di, Y.; Li, J.; Xu, R.; Su, D. S.; Schlögl, R.; Yokoi, T.; Tatsumi, T. *Angew. Chem., Int. Ed.* **2006**, *45*, 3090–3093. (e) White, R. J.; Fischer, A.; Goebel, C.; Thomas, A. *J. Am. Chem. Soc.* **2014**, *136*, 2715–2718. (f) Zhu, J.; Zhu, Y.; Zhu, L.; Rigutto, M.; van der Made, A.; Yang, C.; Pan, S.; Wang, L.; Zhu, L.; Jin, Y.; Sun, Q.; Wu, Q.; Meng, X.; Zhang, D.; Han, Y.; Li, J.; Chu, Y.; Zheng, A.; Qiu, S.; Zheng, X.; Xiao, F. S. *J. Am. Chem. Soc.* **2014**, *136*, 2503–2510.
- (8) (a) Stock, N.; Biswas, S. *Chem. Rev.* **2012**, *112*, 933–969. (b) Morris, R. E.; Bu, X. *Nat. Chem.* **2010**, *2*, 353–361.
- (9) (a) Tian, Y.-Q.; Cai, C.-X.; Ji, Y.; You, X.-Z.; Peng, S.-M.; Lee, G.-H. *Angew. Chem., Int. Ed.* **2002**, *41*, 1384–1386. (b) Choi, E. Y.; Park, K.; Yang, C. M.; Kim, H.; Son, J. H.; Lee, S. W.; Lee, Y. H.; Min, D.; Kwon, Y. U. *Chem.—Eur. J.* **2004**, *10*, 5535–5540. (c) Stavitski, E.; Goesten, M.; Juan-Alcaniz, J.; Martinez-Joaristi, A.; Serra-Crespo, P.; Petukhov, A. V.; Gascon, J.; Kapteijn, F. *Angew. Chem., Int. Ed. Engl.* **2011**, *50*, 9624–9628. (d) Do, X.-D.; Hoang, V.-T.; Kaliaguine, S. *Microporous Mesoporous Mater.* **2011**, *141*, 135–139.
- (10) (a) Bisht, K. K.; Suresh, E. *J. Am. Chem. Soc.* **2013**, *135*, 15690–15693. (b) Zhang, J.; Chen, S.; Nieto, R. A.; Wu, T.; Feng, P.; Bu, X. *Angew. Chem., Int. Ed. Engl.* **2010**, *49*, 1267–1270.
- (11) SAINT, Software Reference Manual; Bruker AXS: Madison, WI, 1998.
- (12) Sheldrick, G. M. *Acta Crystallogr., Sect. A* **2008**, *64*, 112–122.
- (13) Burrows, A. D.; Cassar, K.; Friend, R. M. W.; Mahon, M. F.; Rigby, S. P.; Warren, J. E. *CrystEngComm* **2005**, *7*, 548–550.
- (14) (a) Spek, A. L. *J. Appl. Crystallogr.* **2003**, *36*, 7. (b) Spek, A. L. PLATON, a Multipurpose Crystallographic Tool; Utrecht University: The Netherlands, 2006.
- (15) (a) Zhang, J.; Xue, Y.-S.; Bai, J.; Fang, M.; Li, Y.-Z.; Du, H.-B.; You, X.-Z. *CrystEngComm* **2011**, *13*, 6010–6012. (b) Yang, Q. Y.; Li, K.; Luo, J.; Pan, M.; Su, C. Y. *Chem. Commun.* **2011**, *47*, 4234–4236. (c) Yang, Q.-Y.; Pan, M.; Wei, S.-C.; Hsu, C.-W.; Lehn, J.-M.; Su, C.-Y. *CrystEngComm* **2014**, *16*, 6469–6475. (d) Guo, J.; Yang, J.; Liu, Y.-Y.; Ma, J.-F. *Inorg. Chim. Acta* **2013**, *400*, 51–58.
- (16) (a) Zang, S.; Su, Y.; Li, Y.; Ni, Z.; Zhu, H.; Meng, Q. *Inorg. Chem.* **2006**, *45*, 3855–3857. (b) Haldar, R.; Bonakala, S.; Kanoo, P.; Balasubramanian, S.; Maji, T. K. *CrystEngComm* **2014**, *16*, 4877–4885.
- (17) (a) O’Keeffe, M.; Eddaoudi, M.; Li, H.; Reineke, T.; Yaghi, O. M. *J. Solid State Chem.* **2000**, *152*, 3–20. (b) Carlucci, L.; Ciani, G.; Proserpio, D. M. In *Making Crystals by Design: Methods, Techniques, Applications*; Braga, D., Grepioni, F., Eds.; Wiley-VCH: Weinheim, Germany, 2007; p 58.
- (18) (a) Ruiz-Pérez, C.; Lorenzo-Luis, P.; Hernández-Molina, M.; Laz, M. M.; Delgado, Fernando, S.; Gili, P.; Julve, M. *Eur. J. Inorg. Chem.* **2004**, *2004*, 3873–3879. (b) Lou, Y.; Tao, Y.; Wang, J.; Chen, J.; Ohba, M. *Polyhedron* **2014**, *73*, 72–76.
- (19) Cheary, R. W.; Coelho, A. A. *J. Appl. Crystallogr.* **1992**, *25*, 109–121.
- (20) Li, H.; Eddaoudi, M.; O’Keeffe, M.; Yaghi, O. M. *Nature* **1999**, *402*, 276–279.
- (21) (a) Bordiga, S.; Lamberti, C.; Ricchiardi, G.; Regli, L.; Bonino, F.; Damin, A.; Lillerud, K. P.; Bjorgen, M.; Zecchina, A. *Chem. Commun.* **2004**, 2300–2301. (b) Alvaro, M.; Carbonell, E.; Ferrer, B.; Llabres i Xamena, F. X.; Garcia, H. *Chem.—Eur. J.* **2007**, *13*, 5106–5112. (c) Choi, J. H.; Choi, Y. J.; Lee, J. W.; Shin, W. H.; Kang, J. K. *Phys. Chem. Chem. Phys.* **2009**, *11*, 628–631. (d) Yang, L. M.; Vajeeston, P.; Ravindran, P.; Fjellvag, H.; Tilset, M. *Inorg. Chem.* **2010**, *49*, 10283–10290.
- (22) (a) Zhang, L.; Ma, J.; Yang, J.; Pang, Y.; Ma, J. *Inorg. Chem.* **2010**, *49*, 1535–1550. (b) He, J.; Yu, J.; Zhang, Y.; Pan, Q.; Xu, R. *Inorg. Chem.* **2005**, *44*, 9279–9282.
- (23) (a) Allendorf, M. D.; Bauer, C. A.; Bhakta, R. K.; Houk, R. J. *Chem. Soc. Rev.* **2009**, *38*, 1330–1352. (b) Cui, Y.; Yue, Y.; Qian, G.; Chen, B. *Chem. Rev.* **2012**, *112*, 1126–1162. (c) Wang, X.-S.; Tang, Y.-Z.; Huang, X.-F.; Qu, Z.-R.; Che, C.-M.; Chan, P. W. H.; Xiong, R.-G. *Inorg. Chem.* **2005**, *44*, 5278–5285. (d) Zhai, Q.-G.; Wu, X.-Y.; Chen, S.-M.; Zhao, Z.-G.; Lu, C.-Z. *Inorg. Chem.* **2007**, *46*, 5046–5058.

(e) Zhao, X.; Wang, X.; Wang, S.; Dou, J.; Cui, P.; Chen, Z.; Sun, D.; Wang, X.; Sun, D. *Cryst. Growth Des.* **2012**, *12*, 2736–2739.

(24) Chen, D.-m.; Zhang, X.-p.; Shi, W.; Cheng, P. *Cryst. Growth Des.* **2014**, *14*, 6261–6268.

(25) (a) Lu, Z.; Zhao, W.; Okamura, T.; Fan, J.; Sun, W.; Ueyama, N. *Cryst. Growth Des.* **2007**, *7*, 268–274. (b) Zhu, H.; Wen, L.; Ni, Z.; Li, Y.; Zhu, H.; Meng, Q. *New J. Chem.* **2004**, *28*, 1010–1018. (c) Wang, S.; Xiong, S.; Song, L.; Wang, Z. *CrystEngComm* **2009**, *11*, 896–901.